

FE Modeling of H-SECTION Connecting Rod

Virendra Kumar Verma, Shailendra Kumar, Ashish Gupta

P.G Student, Department of Mechanical Engineering, Babu Banarasi Das University, Lucknow, India

P.G Student, Department of Mechanical Engineering, IIT Bombay, Powai, Mumbai, India

P.G Student, Department of Mechanical Engineering, IIT Bombay, Powai, Mumbai, India

ABSTRACT: This paper describes modeling of H-section connecting rod used for FEA, its generation, simplifications and accuracy. Mesh generation and its convergence are discussed. The load application, particularly the distribution at the contact area, factors that decide load distribution, the calculation of the pressure constants depending on the magnitude of the resultant force, application of the restraints and validation of the FEA model are also discussed. In this paper fatigue in connecting rod is investigated. The investigation is done using ANSYS Workbench 14.0. The reason for performing this research is to locate and analyze the weak point in the design of connecting rod that is affected by reversal loading during its service time.

KEYWORDS: H-section connecting rod, FEA model, ANSYS Workbench 14.0

I. INTRODUCTION

FEA has become an essential step in the design or modeling of a physical phenomenon in various engineering disciplines. A physical phenomenon usually occurs in a continuum of matter (solid, liquid, or gas) involving several field variables. The field variables vary from point to point, thus possessing an infinite number of solutions in the domain. The basis of FEA relies on the decomposition of the domain into a finite number of sub domains (elements) for which the systematic approximate solution is constructed by applying the variational or weighted residual methods. In effect, FEA reduces the problem to that of a finite number of unknowns by dividing the domain into elements and by expressing the unknown field variable in terms of the assumed approximating functions within each element. These functions are defined in terms of the values of the field variables at specific points, referred to as nodes. Nodes are usually located along the element boundaries, and they connect adjacent elements. The ability to discretize the irregular domains with finite elements makes the method a valuable and practical analysis tool for the solution of boundary.

II. FE MODELING OF H-SECTION CONNECTING ROD

This section describes modeling of H-section connecting rod used for FEA, its generation, simplifications and accuracy. Mesh generation and its convergence are discussed. The load application, particularly the distribution at the contact area, factors that decide load distribution, the calculation of the pressure constants depending on the magnitude of the resultant force, application of the restraints and validation of the FEA model are also discussed.

A. MODELING OF H-SECTION CONNECTING ROD

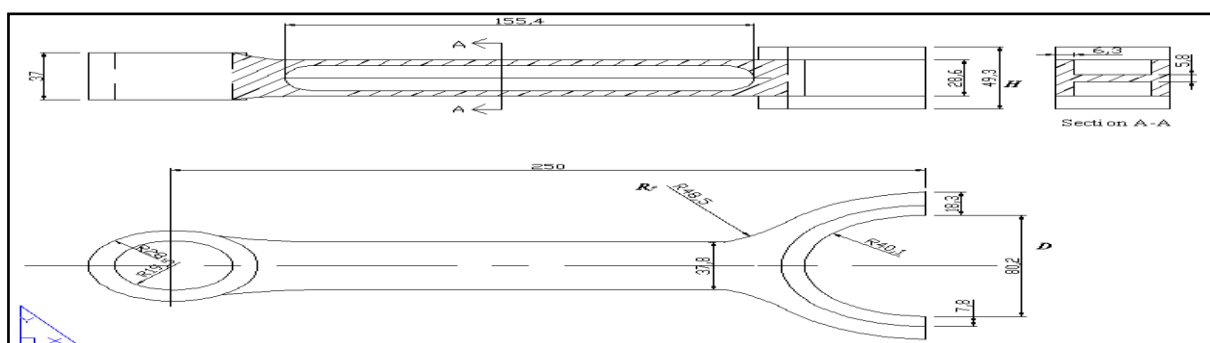


Fig.1 The geometry of the H-section connecting rod[4]

The geometrical dimensions of the H-section connecting rod are shown in Fig.1. The material properties of the connecting rod as shown in Table .1 were used in the FE analysis of the connecting rod for H-section.

A geometrical model of H-section connecting rod as shown in Fig.2 was generated using Pro-E Designing Software. The H-section connecting rod weight as measured on a weighing scale is 1705 grams. The difference in weight between the weights of the solid model used for FEA and the component used by M. Omidet *al* [1], is less than 1%. This is an indication of the accuracy of the solid model. The H-section connecting rod has been modeled keeping the mass of both section constant. A geometrical model of H-section connecting rod as shown in Fig. 4.was generated using Pro-E Designing Software.

Table .1 Properties of the connecting rod used for FE Analysis

Input Parameters	Values
Tensional strength	621 MPa
Yield Strength	483 MPa
Brinell Strength	229-269 HB
Young’s Modulus	207 GPa
Shear Modulus	79 GPa
Poison Ratio	0.3
Density	7.7 Mg/m ³
Correction Coefficient	0.8
Connecting Rod Material	C-70 Alloy steel

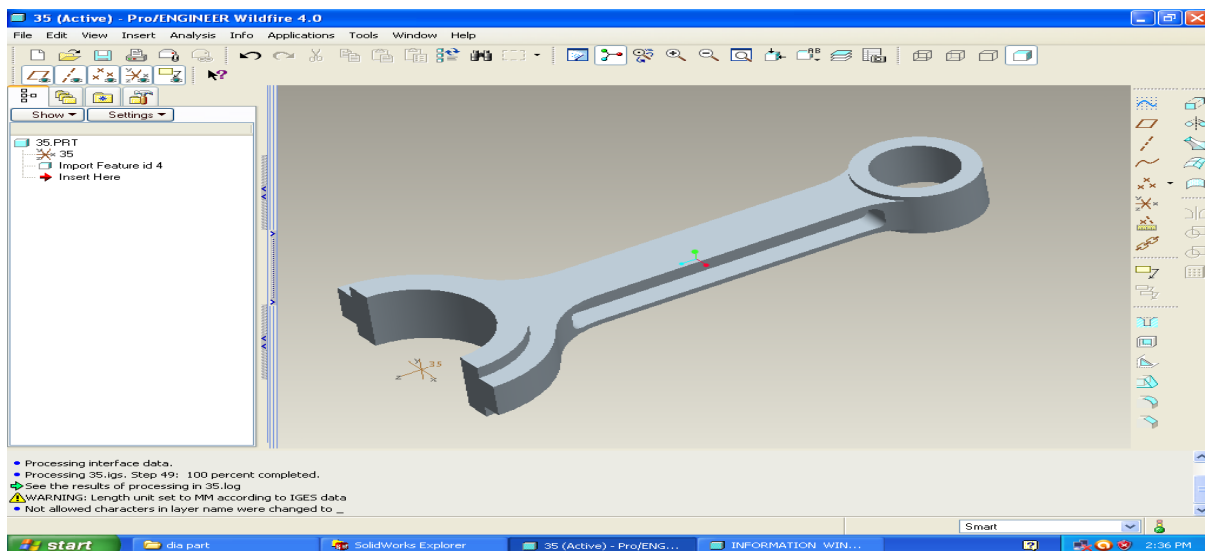


Fig.2 Geometrical Model of H-Section Connecting Rod

In the case of H-section connecting rod, the degree of non-symmetry in the shank region, when comparing the areas on either side of the axis of symmetry perpendicular to the connecting rod length and along the web, was about 5%. This non-symmetry is not the design intent and is produced as a manufacturing variation. Therefore, the connecting rod has been modeled as a symmetric component.

B. MESH GENERATION OF H-SECTION

Pro/E and ANSYS workbench software are used for the FE analysis. The H-section connecting rod was modelled in 3D using Pro/E software, IGES file is generated and then imported in ANSYS workbench software. The next stage was to mesh the connecting rods. The mesh model of H-section was shown in Fig.3. The 10 – node tetragonal elements

(SOLID 187) were used as shown in Fig.4. Finite element mesh was generated using tetragonal elements with element length of 2 mm (2262 elements). The reason for choosing this element was to make the geometrical parts of a complicated mechanical component so enable us to gain more authentic results based on the high techniques of fatigue life calculation.

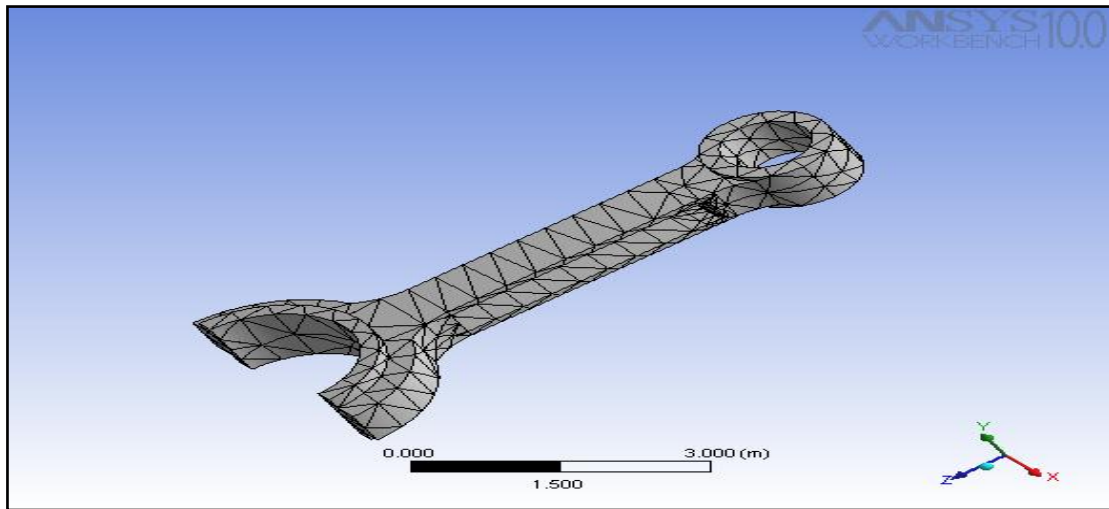


Fig.3 Meshing Model of H-section Connecting Rod

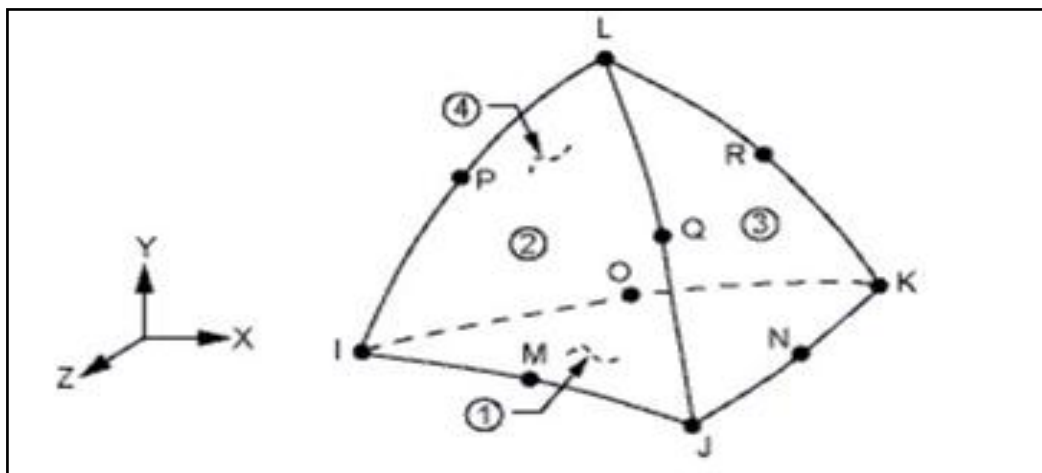


Fig. 4 The 10 – node tetragonal elements (SOLID 187)[5]

SOLID187 element is a higher order 3-D, 10-node element. SOLID187 has quadratic displacement behaviour and is well suited to modelling irregular meshes (such as those produced from various CAD/CAM systems). The element is defined by 10 nodes having three degrees of freedom at each node: translations in the nodal x, y, and z directions. The element has plasticity, hyper elasticity, creep, stress stiffening, large deflection, and large strain capabilities. It also has mixed formulation capability for simulating deformations of nearly incompressible elastoplastic materials, and fully incompressible hyper-elastic materials.

III-BOUNDARY CONDITIONS OF H-SECTION

A. LOADING

The big ends are assumed to have a sinusoidal distributed loading over the contact surface area, under tensile loading, as shown in the Fig.5. This is based on experimental results (Webster *et al.* 1983) [2]. The normal force on the contact surface is given by:

$$F = F_o \cos\theta \dots\dots\dots(1)$$

The load is distributed over an angle of 180°. The total resultant load is given by:

$$F_t = \int_{-\pi/2}^{\pi/2} F_o(\cos^2\theta)rtd\theta = F_o r t \pi / 2 \dots\dots\dots(2)$$

Fig.7 describes r, t and θ . The normal Force constant F_o is, therefore, given by:

$$F_o = F_t / r t \pi / 2 \dots\dots\dots(3)$$

The tensile load acting on the connecting rod, F_t , can be obtained using the expression from the force analysis of the slider crank mechanism.

In this study four finite element models were analyzed. FEA for both tensile and compressive loads were conducted. Two cases were analyzed for each case, one with load applied at the crank end and restrained at the piston pin end, and the other with load applied at the piston pin end and restrained at the crank end. In the analysis carried out, the axial load was 9500 N in both tension and compression. Since the analysis is linear elastic, for static analysis the stress, displacement and strain are proportional to the magnitude of the load. Therefore, the obtained results from FEA readily apply to other elastic load cases by using proportional scaling factor.

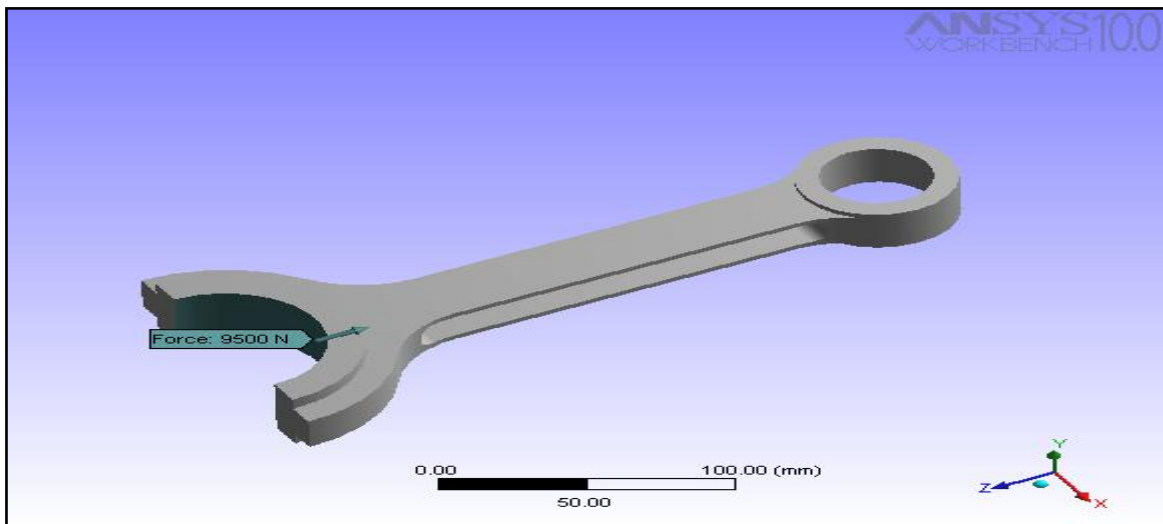


Fig. 5 A sinusoidal distributed loading over the contact surface area, under tensile loading on H-section connecting rod

B. RESTRAINTS

As already mentioned, four FEA models were solved. Fig.6 shows a FEA model in which tensile load is applied at the big end and the small end is restrained. Note that half of the piston pin inner surface (180°) is completely restrained (180° of contact surface area is totally restrained, i.e X, Y, Z translations of all the nodes on this surface are set to zero if the connecting rod is in tension). Similarly, when the connecting rod is under axial compressive load, 120° of contact surface area is totally restrained [3].

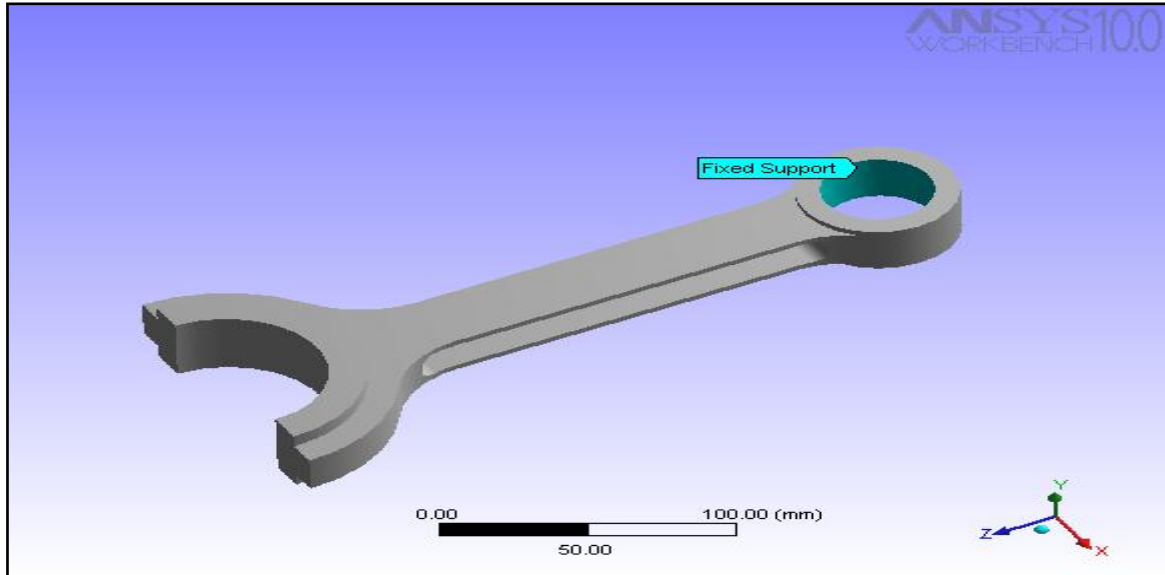


Fig. 6 model in which the small end of H-section connecting rod is restrained

IV. FATIGUE ANALYSIS OF H-SECTION CONNECTING ROD

First of all, the boundary conditions were defined, exerting a tension force. Afterwards, a compressive force, exactly with the same magnitude but in a reverse direction substituted the tension force and it was solved again. In every phase of loading the Von Mises stresses were activated and the critical points were determined.

Fig. 7 shows the stresses generated in the various sector of H-section connecting rod and the critical sector can be observed at the connecting rod stem near the bearing or roundness of big end through the cyclic loading as shown in Fig. 8.

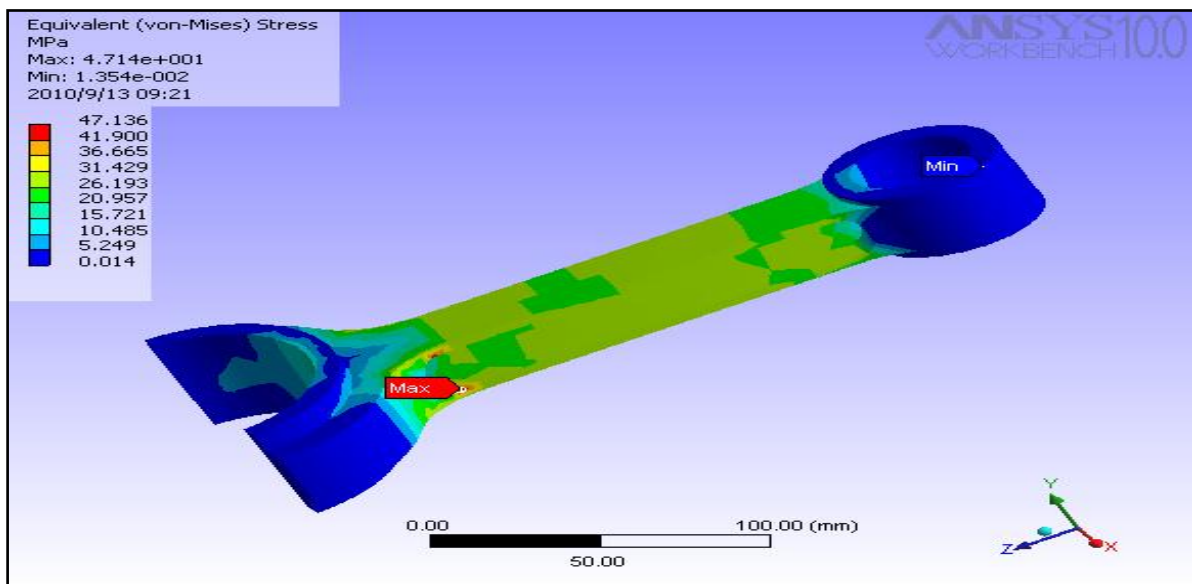


Fig.7 Fatigue Analysis of H-section connection rod

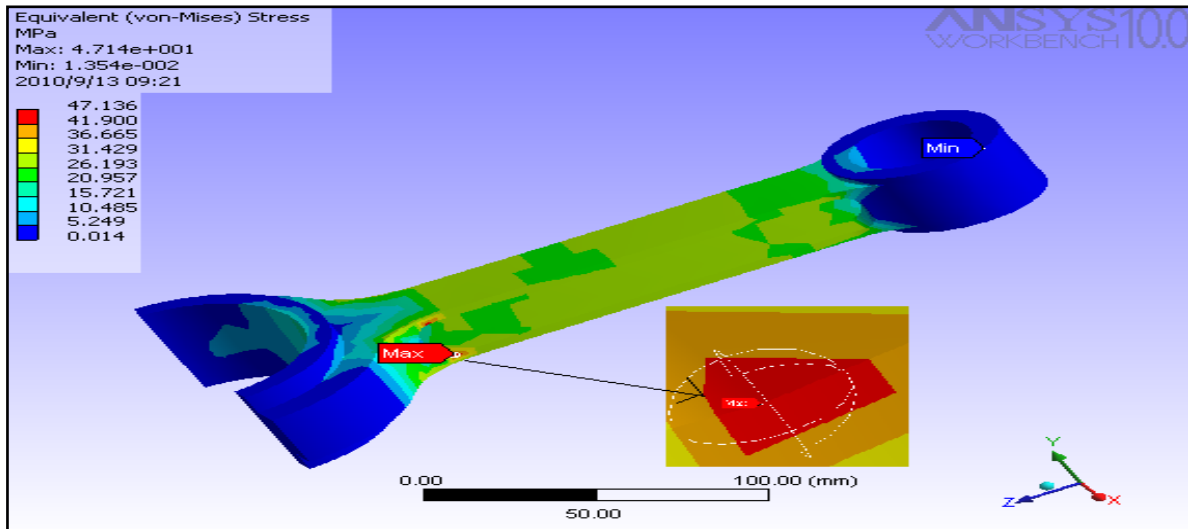


Fig. 8 Critical point of H-section Connecting Rod

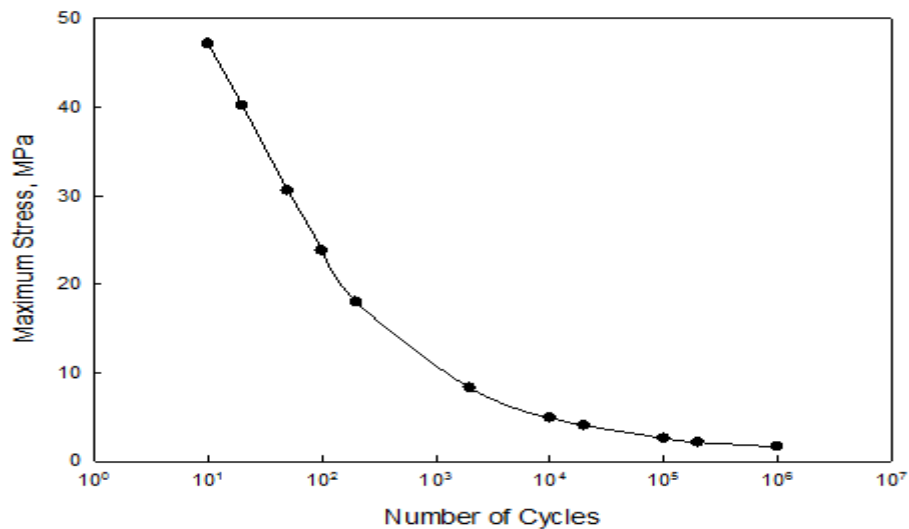


Fig. 9 S-N curve for H-section connecting rod subjected to a fatigue loading

After determination of these critical points, they were elected as the points for fatigue investigation. Filling the fatigue parameter blanks, the S-N data collected from the fatigue test of the specific alloy into the software should import is shown in Fig.9. Eventually a 10⁶ force cycle was exerted to the model and partial consumption rate which indicated the number of exerted cycles to allowable ones for each node was gained. In order to improve and optimize the fatigue life of a connecting rod we can vary some geometrical dimensions keeping all other dimension constant near the big end.

V. VALIDATION OF FINITE ELEMENT ANALYSIS

The properties of the material used for linear elastic finite element analysis are obtained by the M.Omidet *al* [1]. In order to validate the FEA model, the stresses in the shank region half way along the length of the connecting rod were compared under two conditions of compressive load application. First, a 9500 N uniformly distributed load was applied at the big end, while the small end was restrained.

In the present work, the FE analysis for the connecting rod has been carried out using ANSYS workbench software and validate with that obtained by the *Omid et al*[3] and shown in Table 2.

Table 2: Validation of FE Analysis of the connecting rod

Stresses	ANSYS 10	ANSYS Workbench
Maximum Stress in Tension	29.4 MPa	29.94 MPa
Maximum Stress in Compression	24 MPa	23.33 MPa

VI. RESULTS OF H-SECTION CONNECTING ROD

The maximum stress developed in the H-section connecting rod near the big end of the connecting rod is 47.136 MPa. The stresses corresponding to the critical points are calculated by continuously increasing the number of force cycles up to 10^6 .

The remaining figures of present work investigates the effects of critical dimensions, such as fillet radius near the big end (R_f), inner diameter (D) and height of the big end (H), on the mass of the connecting rod and stresses generated at critical point. In the present work, the effect of basic critical dimensions has been investigated on the fatigue life of H-section connecting rod, keeping all other dimensions as constant.

The stresses corresponding to the critical points are calculated by continuously increasing the number of force cycles up to 10^6 . The basic critical dimensions of H-section connecting rod are $R_f = 48.5$ mm, $D = 80.2$ mm and $H = 49.3$ mm [6].

Fig. 10 shows the effect of fillet radius near the big end on the mass of connecting rod, keeping other dimensions constant. It is observed that the mass of connecting rod is proportional to the fillet radius near the big end. As fillet radius increases, the mass of connecting rod also increases and vice-versa.

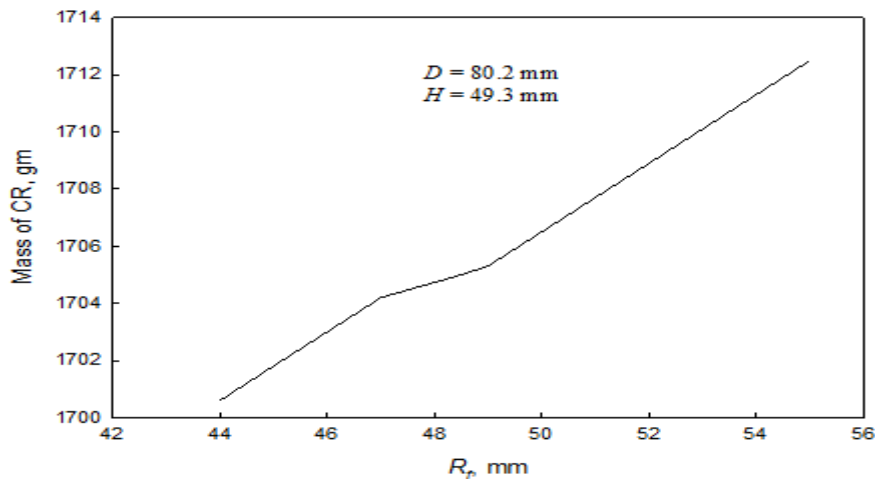


Fig. 10 The effect of fillet radius near the big end on the mass of H-section connecting rod

Fig. 11 shows the effect of big end fillet radius on the maximum stresses generated at the critical point, keeping other dimensions constant. As fillet radius increases or fillet roundness decreases (alternatively, fillet thickness increases due to the additional material), the stress at critical point decreases continuously and after achieving a minimum value it increases slightly and remains constant with further increase in the fillet radius. The basic radius ($R_f = 48.5$) considered in the FE analysis is found to be optimum for the given design. For lower values of fillet radius, below the optimum value of $R_f = 48.5$, the effect of stress concentration is more due to decrease in the thickness of the big end at the critical point.

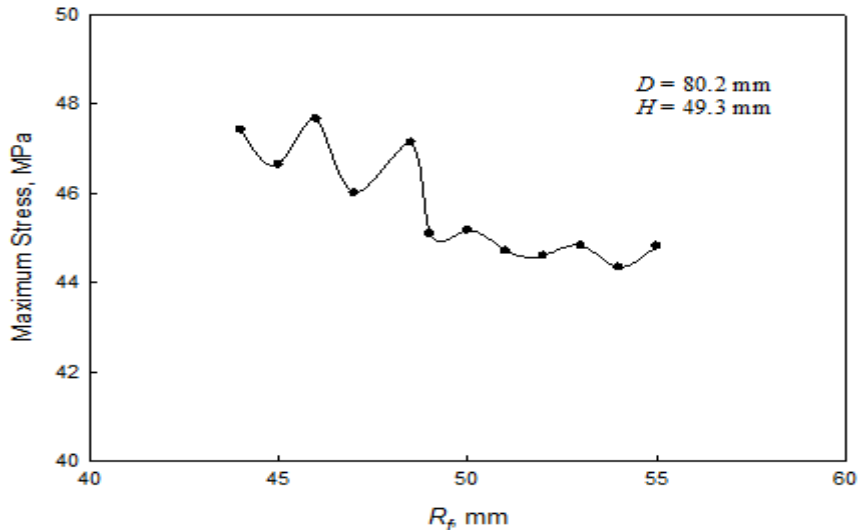


Fig. 11 The effect of big end fillet radius on the maximum stresses generated at the critical point under cyclic loading

Fig. 12 shows the effect of big end inner diameter (D) on the mass of connecting rod, keeping other dimensions constant. As expected, the mass of connecting rod decreases with increase in inner diameter and it is found to be inversely proportional to the inner diameter of the big end. Fig.13 shows the effect of big end inner diameter (D) on the maximum stresses (σ_{max}) generated at the critical point under the cyclic loading. For given fillet radius, the effect of increase in inner diameter slightly decreases the stresses generated at the critical point, and after reaching to a lowest optimum value it increases drastically. It is due to the fact that when thickness of connecting rod at the critical point becomes less than the thickness of remaining circular part of the big end, the section becomes weak very rapidly.

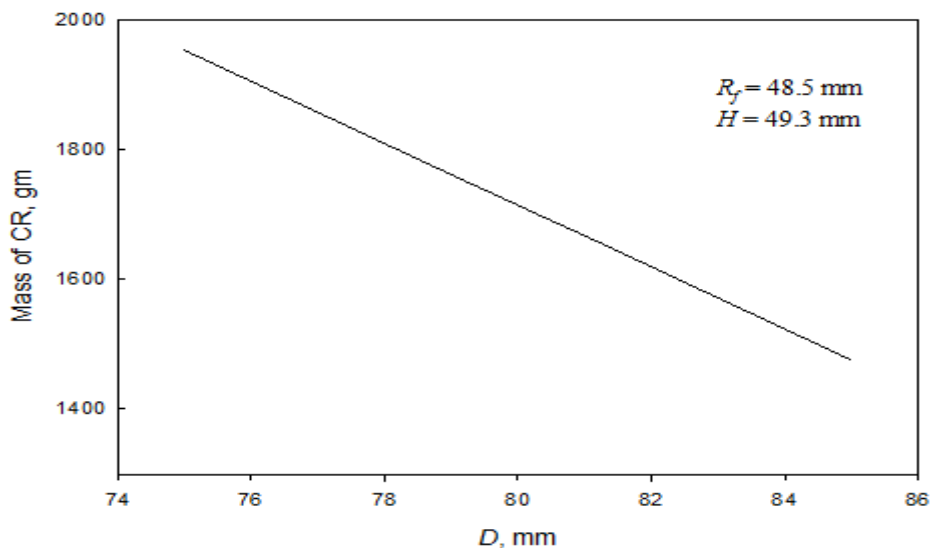


Fig.12 The effect of big end inner diameter (D) on the mass of H-section connecting rod

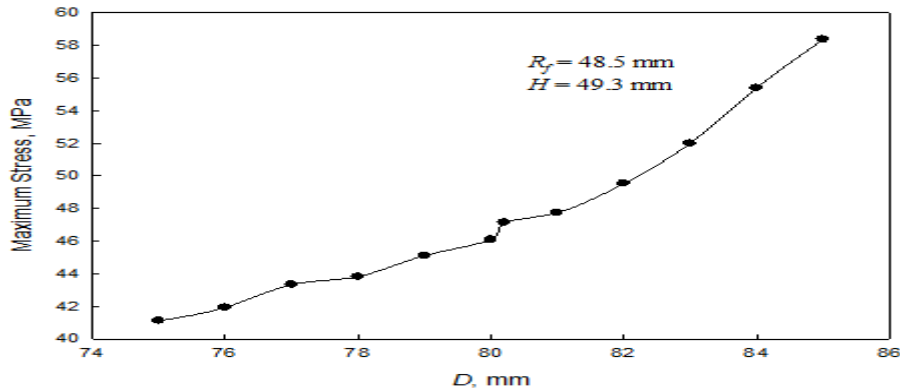


Fig.13 The effect of big end inner diameter (D) on the maximum stresses (σ_{max}) generated at the critical point under the cyclic loading

Fig. 14 shows the effect of height (H) of the big end on the mass of connecting rod, keeping other dimensions constant. It is observed that the mass of connecting rod is proportional to the height of the big end. As height increases, the mass of connecting rod also increases and vice-versa. Fig. 15 shows the effect of height (H) of big end on the maximum stresses generated at the critical point, keeping other dimensions constant. For given fillet radius, the effect of increase in height of big end slightly increases the stresses generated at the critical point, and after reaching to a lowest optimum value it also increases drastically.

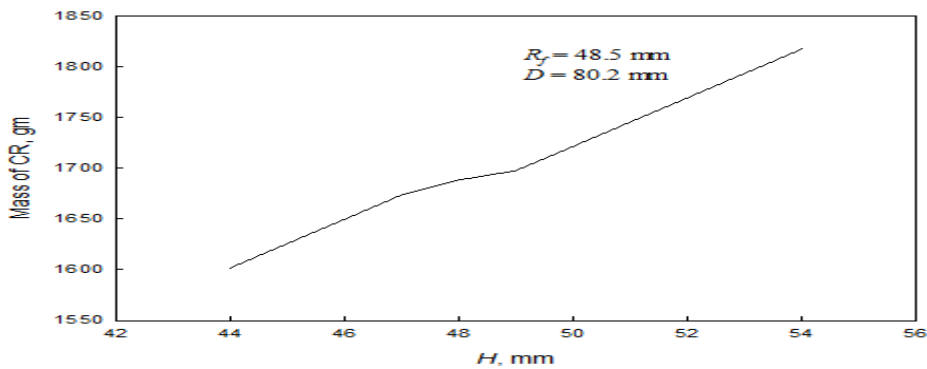


Fig. 14 The effect of height (H) of the big end on the mass of H-section connecting rod, keeping other dimensions constant

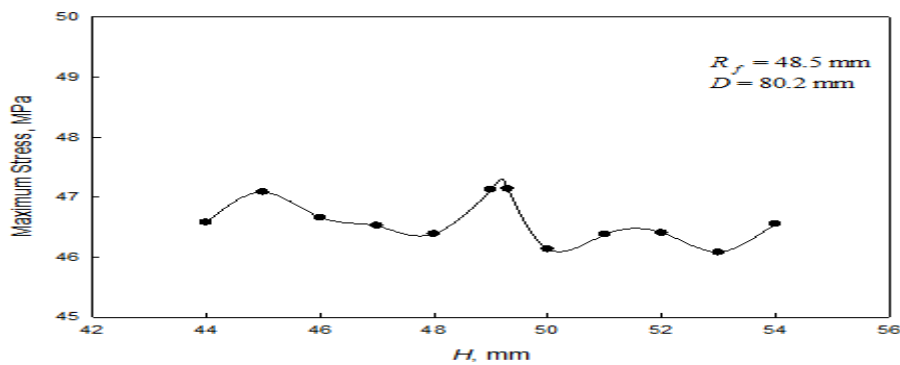


Fig. 15 The effect of height (H) of big end on the maximum stresses generated at the critical point, keeping other dimensions' constant



ISSN: 2350-0328

International Journal of Advanced Research in Science, Engineering and Technology

Vol. 3, Issue 9 , September 2016

VII. CONCLUSION

By the finite element analysis method and the assistance of ANSYS software, it is able to analyze the different components from varied aspects such as fatigue and consequently save the time and the cost. The way that defined loadings was effective on the results achieved. So, they should fit as much as possible the real conditions. As the fatigue analysis requires some static analysis and to define the boundary conditions closest to the real. In this work we conclude that the critical node near the fillet of big end is optimum for all three critical dimensions. This connecting rod design is best suited for manufacturing. Future work will be to comparative study of H-section connecting rod with H-section connecting rod.

REFERENCES

- [1]. M. Omid, S. S. Mohtasebi, S.A. Mireei and F. Mahimoodi, Fatigue Analysis of connecting rod of U650 Tractor in the Finite Element Code ANSYS. 2008.
- [2]. Raymond Browell, "Calculating and Displaying Fatigue Results", Product Manager New Technologies ANSYS, Inc .2006.
- [3]. Whittaker, D., The competition for automotive connecting rod markets. J. Metal Powder Report, VOL-56,PP-32-37,2001.
- [4]. Dr. NWM Bishop and Dr. F. Sherratt, "Finite Element Based Fatigue Calculations" NAFEMS, RLD Ltd., Hutton Roof, Eglinton Rod, Tilford Farnham, Surrey, GU102DH. 2000.
- [5]. Athavale, S. and Sajanpawar, P. R., "Studies on Some Modelling Aspects in the Finite Element Analysis of Small Gasoline Engine Components," Small Engine Technology Conference Proceedings, Society of Automotive Engineers of Japan, Tokyo, pp. 379-389.1991.
- [6]. Rahman, M.M., A.K. Arffin, N. Jamaludin, S. Abdullah and M.M. Noor,. Finite element based fatigue life prediction of a new free piston engine mounting. J. Applied Sci.,vol- 8, pp1612-1621., 2008